Karadeniz Fen Bilimleri Dergisi 8(1), 47-65, 2018

KFBD

Karadeniz Fen Bilimleri Dergisi
The Black Sea Journal of Sciences
ISSN (Online): 2564-7377

Araştırma Makalesi / Research Article

Farklı Kanat Profillerinin Düşük Reynolds Sayısında Planör Aerodinamik Performansı Açısından XFLR5 Kullanılarak Nümerik Olarak İncelenmesi

İbrahim Halil GÜZELBEY[1], Yüksel ERASLAN[2*], Mehmet Hanifi DOĞRU[3]

[1]Gaziantep Üniversitesi, Havacılık ve Uzay Bilimleri Fakültesi, Uçak ve Uzay Mühendisliği Bölümü, Gaziantep, Türkiye
[2]Gaziantep Üniversitesi, Havacılık ve Uzay Bilimleri Fakültesi, Uçak ve Uzay Mühendisliği Bölümü, Gaziantep, Türkiye
[3]Gaziantep Üniversitesi, Havacılık ve Uzay Bilimleri Fakültesi, Pilotaj Bölümü, Gaziantep, Türkiye

[*]**Sorumlu Yazar:** yeraslan@gantep.edu.tr

Geliş Tarihi: 15.05.2018
Kabul Tarihi: 21.05.2018

Özet

Kanat tasarımı, tüm hava araçları için olduğu gibi, planörler için de aerodinamik performans açısından kritik öneme sahiptir. Aerodinamik olarak verimli bir planör kanadı tasarımının en önemli aşamalarından biri de uygun kanat kesit geometrisi (kanat profili) seçimidir. Bir kanat tasarımının kanat kesit geometrisi seçimi, öncelikle belirlenen gerekliliklere dayanarak karşılaştırmak üzere, farklı kanat kesit geometrilerinin aerodinamik performans analizlerini gerektirir. Bu çalışmada, dokuz farklı kanat kesit geometrisi planör aerodinamik performansı açısından karşılaştırmak üzere genel kamu lisanslı XFLR5 programı kullanılarak nümerik olarak incelenmiştir. Öncelikle karşılaştırılacak geometriler Eppler, Goettingen, NACA ve Wortmann kanat kesit geometrisi ailelerinden seçilmiştir. Karşılaştırma için programın deneysel verilerle iki boyutlu doğrulaması yapılmış ve seçilen kanat kesit geometrileri aynı koşullar altında analiz edilmiştir. Analizler $2x10^5$ Reynolds sayısında ve -5 ile 20 derece arasındaki hücum açılarında gerçekleştirilmiştir. Analizlerden elde edilen sonuçlara göre kanat kesit geometrileri belirlenen gereklilikler olan kalınlık, maksimum kaldırma katsayısı ve hücum açısı, maksimum kaldırma durumundaki sürüklenme katsayısı, maksimum süzülme oranı, sıfır kaldırma durumundaki yunuslama momenti ve güç faktörüne göre karşılaştırılmıştır.

Anahtar Kelimeler: Planör, Kanat tasarımı, Kanat kesit geometrisi, XFLR5, Aerodinamik performans.

Numerical Investigation of Different Airfoils at Low Reynolds Number in terms of Aerodynamic Performance of Sailplanes by using XFLR5

Abstract

Wing design has a critical importance for sailplanes as well as for all the aircrafts in terms of aerodynamic performance. One of the important design phases of an aerodynamically efficient sailplane wing is selection of the appropriate airfoil. Airfoil selection of a wing design firstly requires performing aerodynamic performance analyses of different airfoils to compare according to determined requirements. In this study, numerical investigation of nine different airfoils was performed with the aim of comparison in terms of aerodynamic performance of sailplanes by using the general public licensed computer program XFLR5. Firstly, the airfoils which will be compared were selected from Eppler, Goettingen, NACA and Wortmann airfoil families. For the comparison of the airfoils, the two-dimensional analysis validation of the program was done with experimental data, and the airfoils were analyzed in two dimensions under the same validated analysis conditions. The analyses were performed at $2x10^5$ Reynolds number and angle of attacks from -5 to 20 degrees. According to obtained results from the analyses, the airfoils were compared in terms of determined criteria which are thickness, maximum lift coefficient and its angle of attack, maximum drag to lift ratio, drag coefficient at maximum lift condition, pitching moment at zero lift condition and power factor.

Keywords: Sailplane, Wing design, Airfoil, XFLR5, Aerodynamic performance.

This study was presented, in part, at the 3rd International Congress on Mathematic, Engineering and Natural Sciences, Mardin, Turkey, April 2018.

1. Introduction

Sailplanes are the aircrafts, which are aerodynamically streamlined and able to gain altitude while flying in rising air. In three-dimension, as for all aircrafts, wing can be defined as the body, which is the lifting surface of a sailplane. In two-dimension, cross section shape of a wing is named as airfoil. Airfoil shaped body, moving through a fluid, produces aerodynamic forces, which are lift and drag. Airfoil geometry determines the chord-wise lift distribution of a wing. For this reason, one of the important design phases of an aerodynamically efficient sailplane wing is selection of the appropriate airfoil (Thomas and Milgram, 1999).

Airfoil selection of a wing design firstly requires performing aerodynamic performance analysis of different airfoils to compare according to determined requirements. In conceptual design stage of aircrafts, generally it is not preferred to perform expensive and time-consuming wind-tunnel experiments for airfoil analysis. There are many different computer programs and codes, which can perform these analyses quickly and easily. XFOIL (Drela, 1989), XFLR5 (Deperrois, 2009), Eppler Code (Eppler and Somers, 1980) and ANSYS Fluent are some of the well-known programs. For two-dimensional airfoil aerodynamic performance analysis, user-friendly interfaced XFLR5 program uses a fully coupled viscous/inviscid interaction method with a high-order panel method to evaluate drag, boundary layer transition and separation.

In the literature, there are many studies about aerodynamic performance analysis and comparison of airfoils. Hansman and Craig (1987) investigated different airfoils with wind-tunnel experiment conductions. The study includes comparison of three different airfoils in terms of aerodynamic performance degradations under a rain rate. Smith et al. (2008) performed two-dimensional CFD (Computational Fluid Dynamics) analysis for a Wortmann airfoil in ground effect at different angles of attacks. They compared results with data from previous experimental studies and validated that use of this airfoil is useful for a ground effect aircraft in terms of aerodynamic performance. Lasauskas and Naujokaitis (2009) analyzed aerodynamic performances of different airfoils with Eppler Program System, RFOIL and XFOIL. The study includes comparison of codes in terms of accuracy with respect to existing wind-tunnel experimental results at different Reynolds numbers. Wahidi and Bridges (2009) investigated laminar separation bubble behaviours not only at different Reynolds numbers but also at different angle of attacks on NACA 0012 and LA2573 by experimental wind-tunnel analyses. At the end of the study, experimental data of surface pressure distributions compared and found in agreement with the results obtained from XFLR5 program. Xin et al. (2010) performed aerodynamic performance analysis on ANSYS Fluent for a NACA and seagull airfoils at different Reynolds numbers. They found that seagull airfoil is aerodynamically more efficient than the NACA airfoil and proper to use on small-power wind driven generators. Sudhakar

et al. (2011) computed aerodynamic characteristics of a modified version of an existing airfoil geometry, which was obtained using inverse design method of XFLR5 program. With the aim of providing better longitudinal stability for a MAV configuration, they compared aerodynamic performance of the modified airfoil with its original geometry according to XFLR5 analysis results. Vuruşkan et al. (2014) performed aerodynamic performance analysis of VTOL (vertical take-off and landing) aircraft having blended wing body with VLM (vortex-lattice method), NLL (Non-linear numeric lifting line) and CFD (computational fluid dynamics) methods. They used XFLR5 program to obtain airfoil characteristics of airfoils used. They obtained that VLM and CFD methods results in agreement with experimental data existing in literature more than NLL method. Hasan et al. (2017) investigated aerodynamic performances of three airfoils with the help of analysis on Qblade program. With the results of the analysis, mixed airfoil wind turbine blade designed, and its aerodynamic performance investigated with CFD analysis on ANSYS Fluent.

In this study, numerical investigation of nine different airfoils was performed with the aim of comparison in terms of aerodynamic performance of sailplanes by using the general public licensed computer program XFLR5. The airfoils were selected from University of Illinois at Urbana-Champaign's airfoil database (URL-1). For the comparison of the airfoils, seven criteria were selected which are maximum lift coefficient and its angle of attack ($C_{L_{max}}$), maximum drag to lift ratio ($(L/D)_{max}$), performance factor (${C_L}^{3/2}/C_D$), zero lift pitching moment (C_{M_0}), thickness and drag coefficient (C_D). For the reliability verification of the program results, firstly it was observed that obtained analysis results of XFLR5 for an airfoil were in admissible agreement with experimental data. After the validation, Eppler E603, NACA 23012, Wortmann FX S-02-196, Wortmann FX 73-K170, Wortmann FX 60-126, Wortmann FX 61-184, Wortmann FX 62-K-153, Goettingen 533 and Goettingen 549 airfoils were analyzed in two dimensions by using the same analysis conditions. The analyses were performed at selected wide range of angle of attack from -5 to 20 degrees and $2x10^5$ Reynolds number. Consequently, according to results, which were obtained from the analyses, airfoils were compared in terms of the determined criteria.

2. Material and Method

2.1. Airfoil Geometry

In three-dimension, as for all aircrafts, wing can be defined as the body, which is the lifting surface of a sailplane. In two-dimension, cross section shape of a wing is named as airfoil and usually identified with geometrical terms as defined in Figure 1. The line drawn horizontally from leading to trailing edge of the airfoil is named as chord-line. The mean-camber is the line that determines amount

of the curvature of the airfoil with respect to its upper and lower surfaces. The airfoil is called as symmetrical if the mean-camber and chord-line of an airfoil are intersected. Additionally, maximum thickness is another important parameter that describes the airfoil geometry. Its value and its distance from the leading edge is generally described as a percentage of the airfoil chord-line length.

In general, for sailplane wing designs, it is desirable for an airfoil to be as thin as possible at the tip section because airfoils, which have smaller maximum thickness value, produces lower induced drag. Also, for sailplane wing designs, generally it is desirable for root section airfoil to be as thick as possible because of needed structural strength and needed volume for water ballast tanks (Thomas and Milgram, 1999; Gudmundsson, 2013).

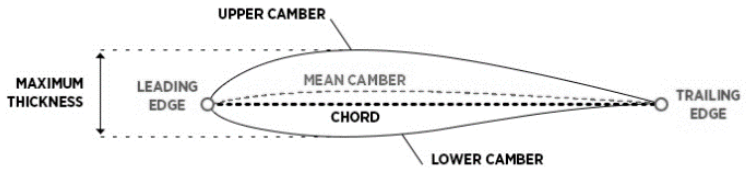

Figure 1. An airfoil geometry

In this study, nine different non-symmetrical airfoil geometries were selected from University of Illinois at Urbana-Champaign's database (URL-1). The selected airfoils, whose geometries are given in Figure 2, are Eppler E603, NACA 23012, Wortmann FX S-02-196, Wortmann FX 73-K170, Wortmann FX 60-126, Wortmann FX 61-184, Wortmann FX 62-K-153, Goettingen 533 and Goettingen 549.

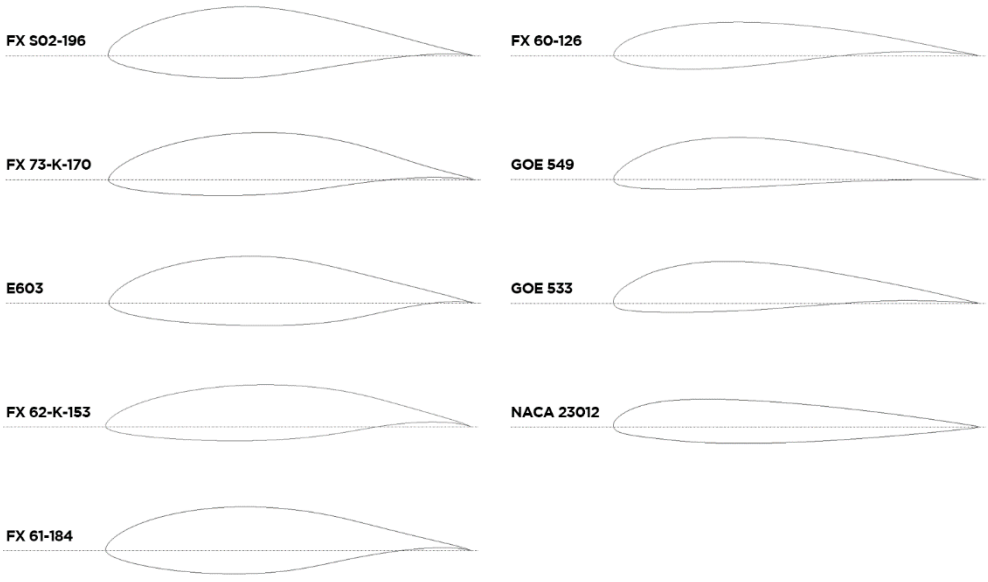

Figure 2. Selected airfoil geometries

Historical usage data shows not only frequent usage of the selected airfoils but also their application trends at root or tip sections of sailplane wing designs. By means of this data, the selected airfoils were divided into two groups as stated in Table 1.

Table 1. Groups of Selected Airfoils

Root Section Airfoils	Max. Thickness	Tip Section Airfoils	Max. Thickness
Eppler E603	19%	Goettingen 533	13,82%
Wortmann FX S-02-196	19,6%	Goettingen 549	13,85%
Wortmann FX 73-K170	17%	NACA 23012	12%
Wortmann FX 61-184	18,4%	Wortmann FX 60-126	12,6%
Wortmann FX 62-K-153	15,3%		

2.2. XFLR5

XFLR5 is a user-friendly design and analysis program for airfoils and bodies. The program uses XFOIL codes for two-dimensional airfoil aerodynamic performance analysis. The program is capable of calculating lift, drag, pitching moment and pressure coefficients of airfoils in two-dimension by using fully coupled viscous/inviscid interaction method with high-order panel method.

2.2.1. Inviscid Analysis

XFLR5 inviscid analysis in two-dimension has a linear-vorticity streamfunction formulation. For the analysis, the program constructs an inviscid airfoil flowfield in two-dimension. This flowfield consists of not only a freestream flow but also a vortex sheet on the airfoil together with a source sheet on the wake and airfoil surface. Thus, streamfunction can expressed as

$$\Psi(x,y) = u_\infty - v_\infty + \frac{1}{2\pi}\int \gamma(s) lnr(s;x,y) + \frac{1}{2\pi}\int \sigma(s)\theta(s;x,y)ds \quad (1)$$

where σ is source sheet strength, γ is vortex sheet strength, s is the coordinate through the vortex and source sheets, $v_\infty = q_\infty sin\alpha$ and $u_\infty = q_\infty cos\alpha$ are freestream velocity components, r is the magnitude of the vector between the field point x, y and the point s and θ is the angle of the vector.

The airfoil surface and wake trajectory are both divided into a number of flat panels. As shown in Figure 4, the number of panel nodes on the airfoil is N and the number of panel nodes on the wake is N_w. There are linear vorticity distributions (γ_i) at each airfoil panel. Additionally, there is a constant source strength (σ_i) for each airfoil and wake panel associated with them.

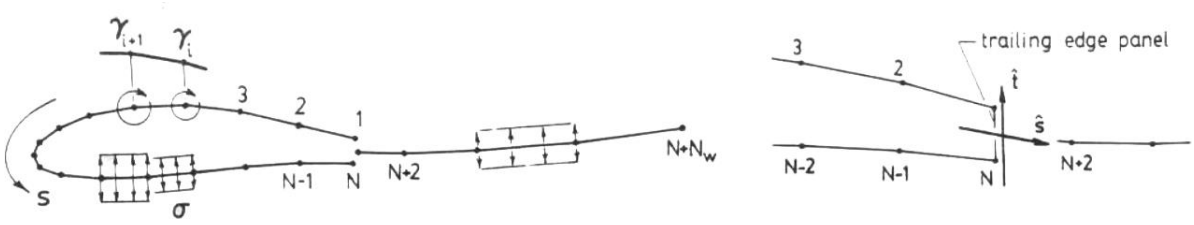

Figure 4. Vorticity and source distributions and panels of airfoil and wake

Defining the unit streamfunctions with local panel coordinates and equaling the streamfunction Ψ_0, which has some constant value, at each node on the airfoil gives equation (2)

$$\sum_{j=1}^{N}\left(a_{i,j}\gamma_j\right) - \Psi_0 = -u_\infty y_i + v_\infty x_i - \sum_{j=1}^{N+N_w-1}\left(b_{i,j}\sigma_{0,j}\right) \qquad ; \qquad 1 \le i \le N \tag{2}$$

where $a_{i,j}$ and $b_{i,j}$ are the coefficient matrices and x_i and y_i are airfoil panel nodes. Combining linear system with Kutta condition, which means equaling sum of the strengths of vortex panels at trailing edge nodes to zero, gives equation (3)

$$\gamma_1 + \gamma_N = 0 \tag{3}$$

which is a linear system with N+1 equations and N+1 unknown values of γ_i. Inside the airfoil, the flow is stagnant. Hence, the surface velocity is equal to surface vorticity and expressed as

$$\gamma_i = q_i \tag{4}$$

where q_i is surface velocity. Hence, pressure coefficient can be expressed with respect to surface vorticity by applying Bernoulli's equation

$$C_p = 1 - \left(\frac{\gamma}{q_\infty}\right)^2 \tag{5}$$

where freestream velocity is $q_\infty = \sqrt{{v_\infty}^2 + {u_\infty}^2}$.

2.2.2. Viscous Analysis

For a viscous analysis with a known airfoil geometry, XFLR5 program gives solution for airfoil surface vorticity by solving matrix equation (2) and Kutta condition (3) by means of Gaussian elimination as

$$\gamma_i = \gamma_{0i} cos\alpha + \gamma_{90i} sin\alpha + \sum_{j=1}^{N+N_w-1} \left(b'_{i,j}\sigma_{0,j}\right) \quad ; \quad 1 \leq i \leq N \tag{6}$$

where γ_0 and γ_{90} are the vorticity distributions, which is a freestream α of 0 and 90 degrees. $b'_{i,j} = -a^{-1}_{i,j} b_{i,j}$ is the source influence matrix. For viscous flows, the boundary layer equations should be added to the equation (4) to obtain solvable closed system because of the source strengths are unknown (Drela, 1989).

2.2.3. XFLR5 Two-dimensional Analysis Validation

For the reliability verification of XFLR5 two-dimensional viscous analysis results, an analysis was performed on Eppler E387 airfoil at the same conditions with wind tunnel experiment results at Langley Low-turbulence Pressure Tunnel (McGhee et al., 1988). XFLR5 analyses were performed at $2x10^5$ Reynolds number and 0.06 Mach number, which was same as the reference experimental study. As it is observed by Morgado et al. (2016), to define an airfoil in XFLR5, using more than 150 number of panels does not show an important difference in the results. Although it is enough to use 150 number of panels, it is selected to use 250 panels as performing analyses takes very little time for XFLR5.

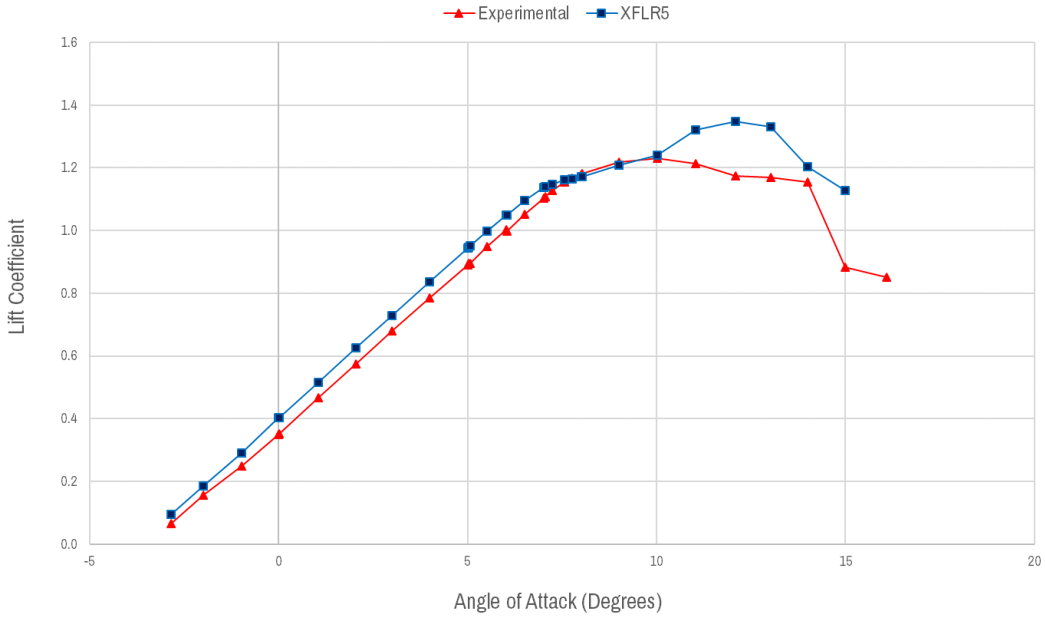

Figure 5. Comparison of experimental results with XFLR5 analysis results in terms of lift coefficient changing with angle of attack

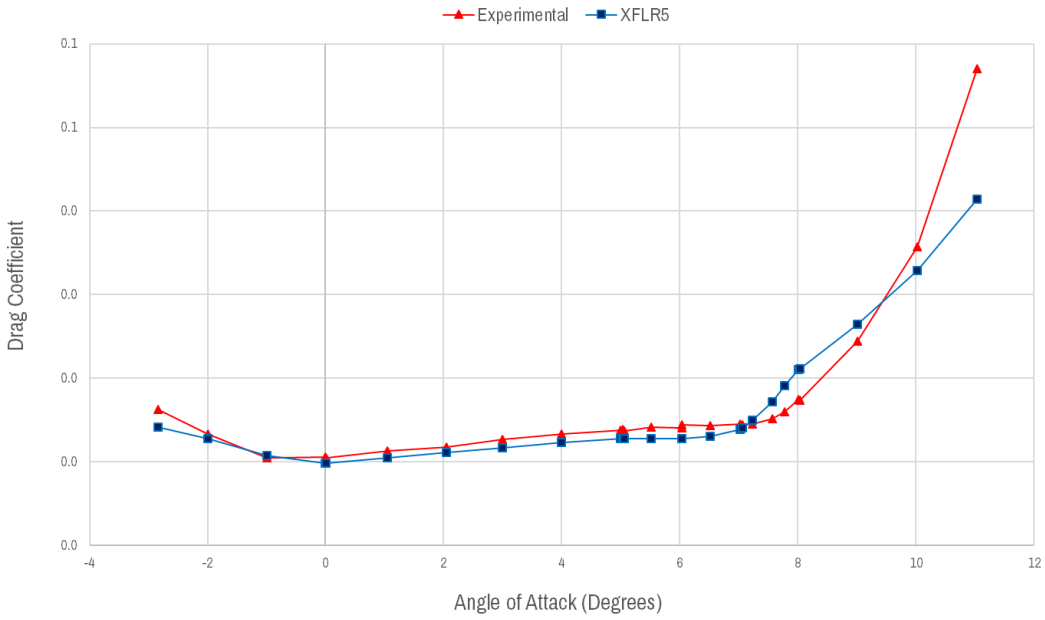

Figure 6. Comparison of experimental results with XFLR5 analysis results in terms of drag coefficient changing with angle of attack

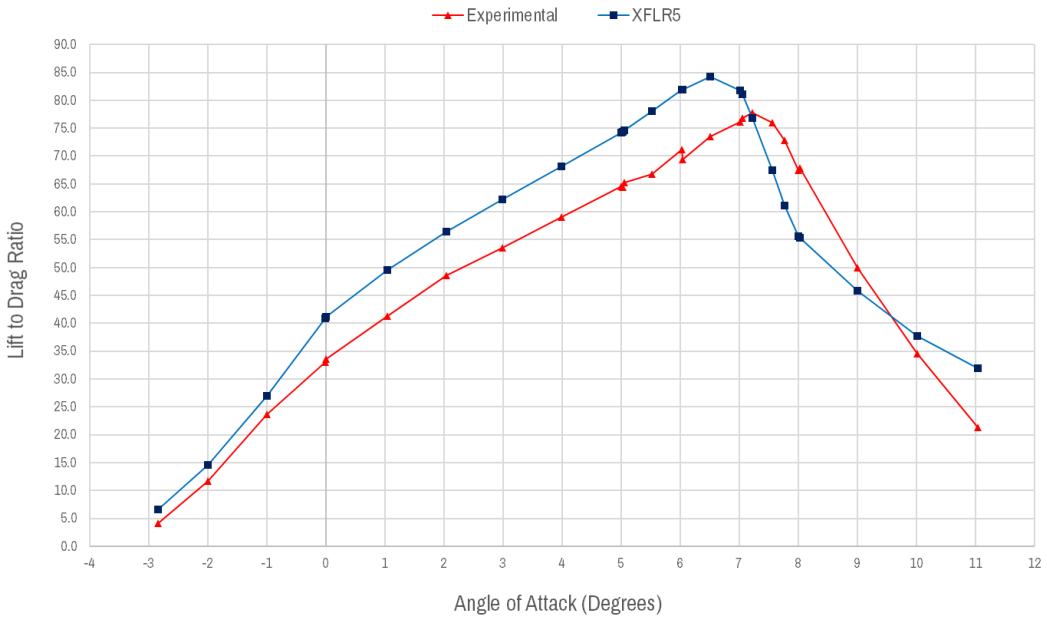

Figure 7. Comparison of experimental results with XFLR5 analysis results in terms of lift to drag ratio changing with angle of attack

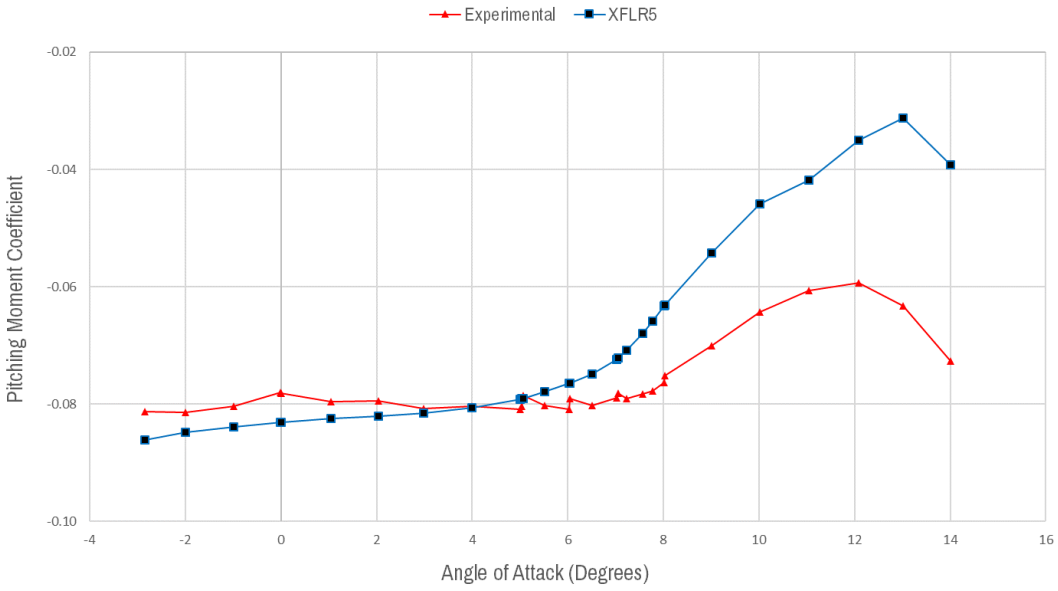

Figure 8. Comparison of experimental results with XFLR5 analysis results in terms of pitching moment coefficient changing with angle of attack

As a result of the analyses, Figure 5 and Figure 6 shows that XFLR5 gives very close lift coefficient and drag coefficient results to experimental data up to stall angle of attack, which is 10 degrees. Lift and drag coefficients results of XFLR5 and experimental data have difference lower than 10 percent in average. As it can be clearly seen in Figure 7, lift to drag ratio results of XFLR5 and experimental data have difference lower than 15 percent in average. Additionally, maximum lift

to drag ratio is 8.3 percent more than the experimental data. Figure 8 indicates that, pitching moment coefficient results of XFLR5 are compatible with experimental data. In average, their difference is lower than 15 percent in terms of their values. At low angle of attacks, XFLR5 gives very close results to experimental data with difference lower than 6 percent.

Consequently, it was obtained that, XFLR5 gives results whose difference is lower than 10 percent in average from experimental data in terms of drag, lift and pitching moment coefficients.

2.4. Aerodynamic Parameters

2.4.1. Lift, Drag and Pitching Moment Coefficients

A body moving through a fluid causes two forces to be created which are named as drag and lift. Lift force is perpendicular and drag force is parallel to the relative airflow direction. General lift force, drag force and pitching moment formulas are stated in equations (7), (8) and (9).

$$L = \frac{1}{2}\rho A V^2 C_L \tag{7}$$

$$D = \frac{1}{2}\rho A V^2 C_D \tag{8}$$

$$M = \frac{1}{2}\rho A V^2 C_M c \tag{9}$$

where L is the lift force, M is the pitching moment, D is the drag force, A is the reference area, c is the chord-length, V is the velocity, ρ is the fluid density and C_L, C_M and C_D are the lift, pitching moment and drag coefficients, respectively.

Maximum lift coefficient directly affects the minimum velocity of the sailplane. Hence, for a sailplane wing, it is desirable to have highest maximum lift coefficient at highest possible angle of attack ($\alpha_{C_{L_{max}}}$). This makes the wing to have lower stall speed and stall angle of attack. Also, having minimum drag coefficient at maximum lift condition provides good thermaling performance for sailplanes (Thomas and Milgram, 1999).

Lift to drag ratio, as stated in equation (10), is an important parameter for sailplanes, which is also named as efficiency or glide ratio. It is the ratio between the horizontal travelled distance and loss of altitude in a given time. Hence, the higher the glide ratio, the higher the sailplane aerodynamic efficiency (Thomas and Milgram, 1999).

$$E = \frac{L}{D} = \frac{C_L}{C_D} \quad (10)$$

There is another important parameter called as index of stability, which is the moment coefficient for zero lift condition (C_{M_0}). Sailplane is said to be stable if C_{M_0} has negative value. Additionally, stability increases if C_{M_0} has closer value to zero (Frati, 1946).

For sailplanes, it is desirable to have low power required to maintain flight and low sink velocity. There is a parameter which measures the quality of climb and the velocity of sink named as climb index or power factor ($C_L{}^{3/2}/C_D$). The higher value of this factor lowers the sink velocity and the power required to maintain flight (Thomas and Milgram, 1999).

2.4.2. Reynolds Number and Mach Number

Reynolds number is a dimensionless parameter, which is equal to division of inertial and viscous forces as stated in equation (11). This parameter determines whether the flow is laminar or turbulent. It can be defined as

$$Re = \frac{inertial\ force}{viscous\ force} = \frac{\rho V L}{\mu} \quad (11)$$

where ρ is the fluid density, V is the flow velocity, L is the characteristic length, and μ is dynamic viscosity of the fluid. Mach number is the ratio of the speed of a body to the speed of sound in the fluid that body travels. It can be defined as

$$M = \frac{V_0}{V_s} \quad (12)$$

where V_0 is the speed of the body and V_s is speed of the sound. If the mach number is lower than 1, the speed is named as subsonic.

3. Results and Discussion

Analyses were performed on XFLR5 at 2x10^5 Reynolds number and from -5 to 20 degrees with 0.5 degree intervals. For selected tip section airfoils, depending on changing angle of attack; lift coefficient, drag coefficient, lift to drag ratio, pitching moment coefficient and power factor diagrams

were shown in Figure 9, 10, 11, 12 and 13, respectively. The diagrams including same parameters were given for the root section airfoils in Figure 14, 15, 16, 17 and 18.

In Figure 9 and 14, it is observed that, lift coefficient of each airfoil increased up to different angle of attacks and decreased after their peak values. For the selected airfoils, it can be clearly seen in Table 2, FX 73-K170 and FX 60-126 airfoils have the maximum $C_{L_{max}}$ value among their groups, which were root and tip section airfoils. Regarding to flight mechanics, higher $C_{L_{max}}$ refers lower stall speed for a wing. Hence, these two airfoils were found to provide lower stall speeds among the other selected airfoils. Moreover, angle of attack of maximum lift condition ($\alpha_{C_{L_{max}}}$) is another important parameter that determines stall angle of attack. The higher the $\alpha_{C_{L_{max}}}$, the higher the stall angle of attack of a wing. In Table 2, it was obtained that E603 and FX 60-126 airfoils have the maximum values of $\alpha_{C_{L_{max}}}$. Hence, these two airfoils were found to provide maximum stall angle of attack among the other selected airfoils.

In Figure 10 and 15, as expected, drag coefficient of each airfoil varied a little up to different angle of attacks and later on increased suddenly in a short angle of attack interval. At maximum lift condition, drag coefficients of the selected airfoils were given in Table 2. Having smaller drag coefficient at maximum lift condition is important in terms of thermaling performance of sailplanes. As it was stated in Table 2, FX 62-K-153 has the minimum value of drag coefficient at maximum lift condition among the root section airfoils. Additionally, at the maximum lift condition, GOE 549 has the minimum drag coefficient value among the tip section airfoils. Thus, these two airfoils were found the most efficient airfoils among the selected airfoils in terms of thermaling performance.

In Figure 13 and Figure 18, diagrams of the power factors of the airfoils were given changing with angle of attack. Higher power factor means lower power required to maintain flight and lower sink rate. From the results, it was obtained that, FX 62-K-153 and GOE 533 airfoils has the maximum power factor values among the others. So, these two airfoils were found the most efficient airfoils among the other selected airfoils in terms of power factor.

Figure 11 and 16 shows that, each airfoil has increasing lift to drag ratio up to different angle of attacks. Later on, it was seen that, after the peak value, glide ratio decreased with the increasing angle of attack for all the selected airfoils. For sailplanes, lift to drag ratio is a parameter, which determines the aerodynamic efficiency. The higher the glide ratio, the higher the horizontal distance travelled in a time interval, which has a crucial importance for sailplanes. It can be clearly seen in Table 3, FX 62-K-153 and FX 61-184 airfoils have the maximum glide ratios among the other root and tip section airfoils, respectively. Hence, these two airfoils were found the most efficient airfoils among the selected airfoils in terms of lift to drag ratio.

As it is observed in Figure 12 and 17, except for NACA 23012, each of the airfoils has negative values for entire of the angle of attack interval. Zero lift pitching moment coefficient has an important role on sailplane stability. If C_{M_0}has a negative value, sailplane is said to be stable. Also, stability increases if C_{M_0} has closer value to zero. It was observed from Table 2, E603 and NACA 23012 airfoils has not only negative, but also the closest C_{M_0} values to zero. Hence, these two airfoils were found to be most suitable in terms of stability.

As it is stated before, for tip section airfoils, it is desirable to have smaller maximum thickness value because thin airfoils produces lower induced drag. Oppositely, the root section airfoils desired to be as thick as possible because of needed structural strength and volume for water ballast tanks.

Taking results of the analyses into consideration, all of the selected root and tip section airfoils were scored from 1 to 5 according to the determined criteria, as stated in Table 4 and Table 5.

Table 2. Analysis Results for Each Airfoil in terms of Maximum Lift Coefficient and Its Angle of Attack, Pitching Moment Coefficient at Zero Lift Condition and Drag Coefficient at Maximum Lift Condition

Airfoil Name	$C_{L_{max}}$	$\alpha_{C_{L_{max}}}$(degree)	$C_D\ at\ C_{L_{max}}$	C_{M_0}
E603	1.34	12	0.2920	-0.0712
FX S02-196	1.38	10	0.0226	-0.098
FX 61-184	1.40	10.5	0.0253	-0.1018
FX 73-K-170	1.44	11	0.0284	-0.1045
FX 62-K-153	1.36	8.5	0.02	-0.1315
NACA 23012	1.31	13.5	0.037	-0.0079
GOE 533	1.62	13	0.033	-0.0112
GOE 549	1.53	12.5	0.028	-0.1034
FX 60-126	1.55	14	0.052	-0.1177

Table 3. Analysis Results for Each Airfoil in terms of Maximum Glide Ratio and Its Angle of Attack

Airfoil Name	$(L/D)_{max}$	$\alpha_{(L/D)_{max}}$(degree)	$({C_L}^{3/2}/C_D)_{max}$
E603	58.1	10.5	66.8
FX S02-196	68.6	8.5	79.6
FX 61-184	69.9	8.5	81.5
FX 62-K-153	76.7	7.5	88.5
FX 73-K-170	62.4	8.5	76.2
NACA 23012	51.1	9.5	55.4
GOE 533	74.1	8	88.6
GOE 549	74.3	7.5	86.7
FX 60-126	79.6	5.5	85.2

Table 4. Root Section Airfoils Comparison Scores

Airfoil Name	$(L/D)_{max}$	$C_{L_{max}}$	$\alpha_{C_{L_{max}}}$	$C_D\ at\ C_{L_{max}}$	$({C_L}^{3/2}/C_D)_{max}$	C_{M_0}	Thickness	AVERAGE
E603	1	1	5	1	1	5	4	2.57
FX S02-196	3	3	2	4	3	4	5	3.43
FX 61-184	4	4	3	3	4	3	3	3.43
FX 73-K-170	2	5	4	2	2	2	2	2.71
FX 62-K-153	5	2	1	5	5	1	1	2.86

Table 5. Tip Section Airfoils Comparison Scores

Airfoil Name	$(L/D)_{max}$	$C_{L_{max}}$	$\alpha_{C_{L_{max}}}$	$C_D\ at\ C_{L_{max}}$	$({C_L}^{3/2}/C_D)_{max}$	C_{M_0}	Thickness	AVERAGE
NACA 23012	1	1	3	2	1	4	4	2.29
GOE 533	2	4	2	3	4	3	2	2.86
GOE 549	3	2	1	4	3	2	1	2.29
FX 60-126	4	3	4	1	2	1	3	2.57

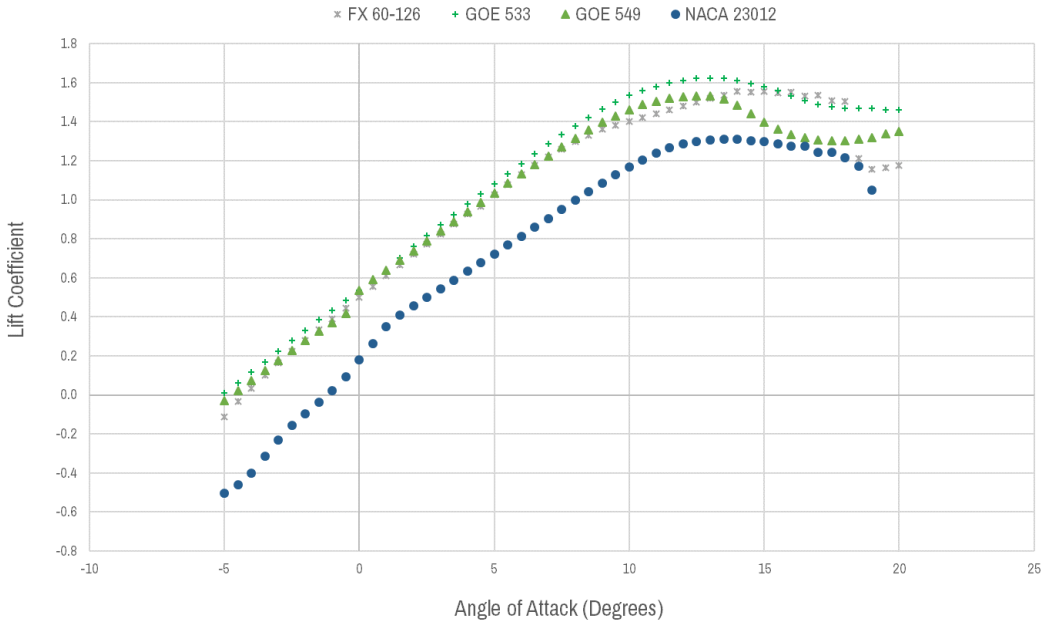

Figure 9. Lift coefficients of tip section airfoils changing with angle of attack

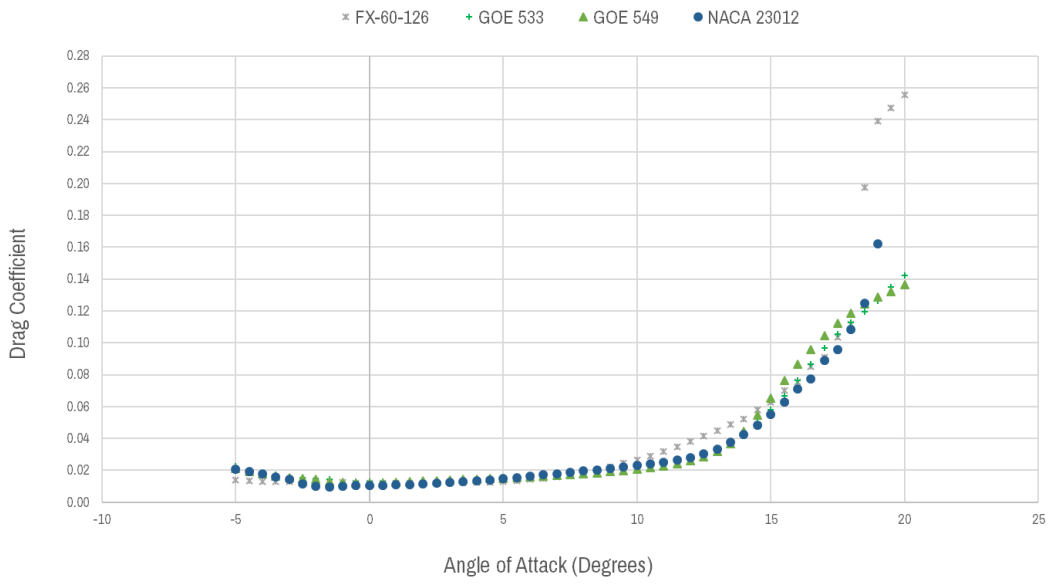

Figure 10. Drag coefficients of tip section airfoils changing with angle of attack

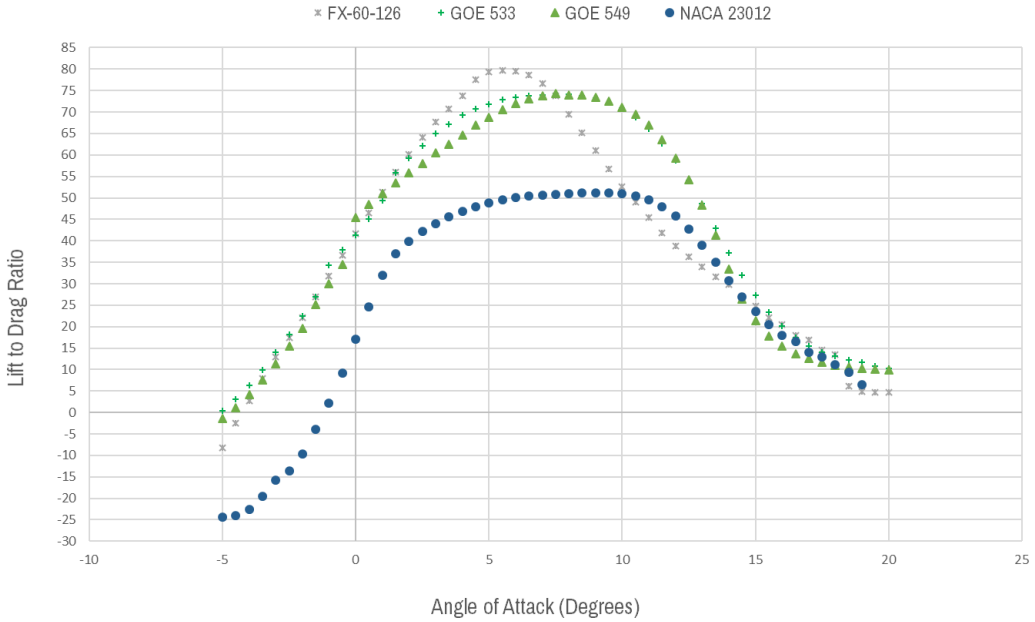

Figure 11. Lift to drag ratios of tip section airfoils changing with angle of attack

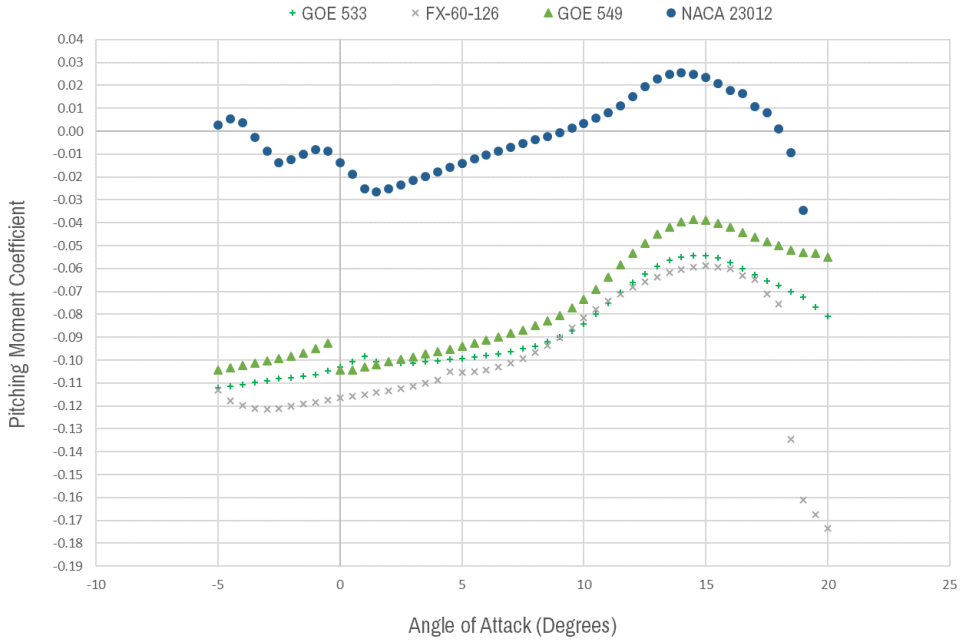

Figure 12. Pitching moment coefficients of tip section airfoils changing with angle of attack

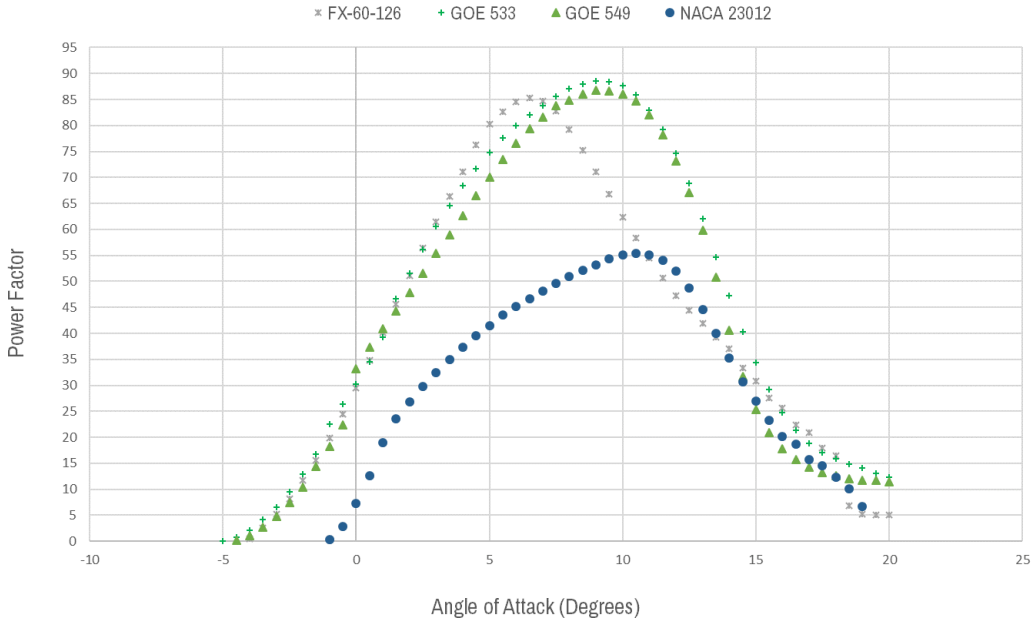

Figure 13. Power factors of tip section airfoils changing with angle of attack

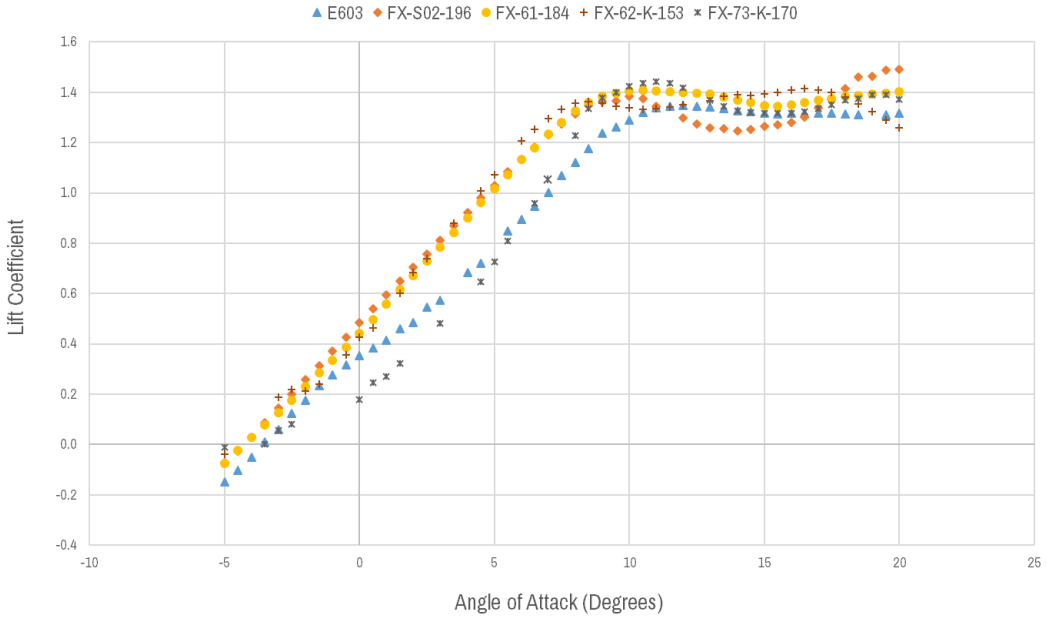

Figure 14. Lift coefficients of root section airfoils changing with angle of attack

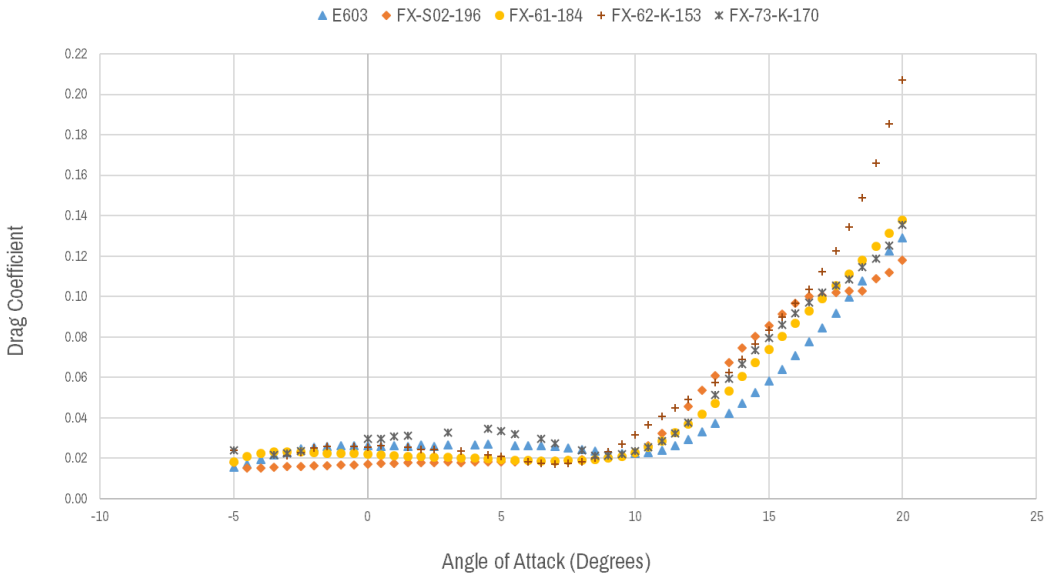

Figure 15. Drag coefficients of tip section airfoils changing with angle of attack

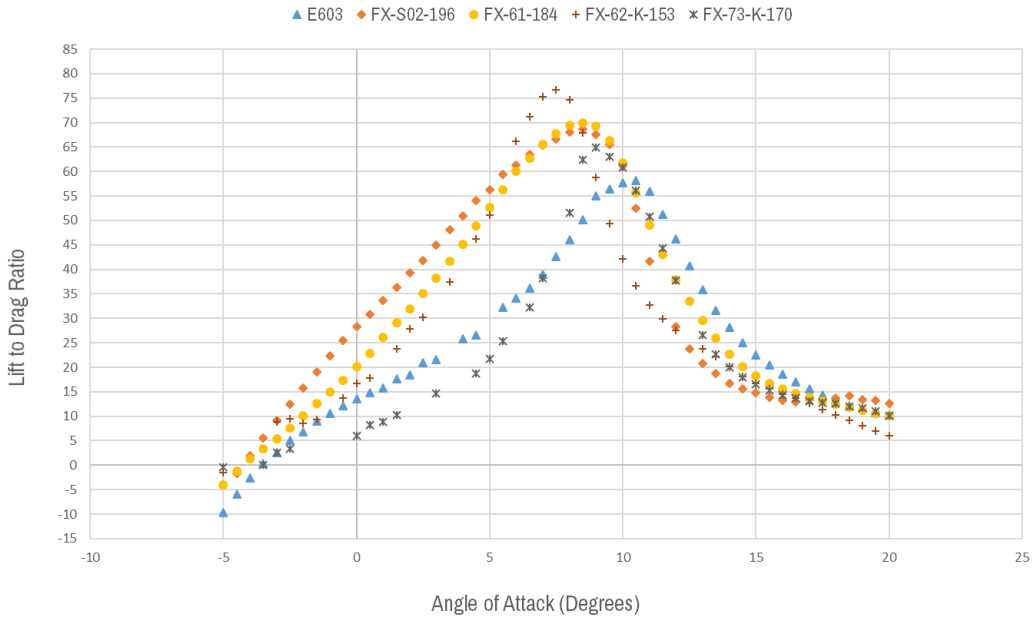

Figure 16. Lift to drag ratios of tip section airfoils changing with angle of attack

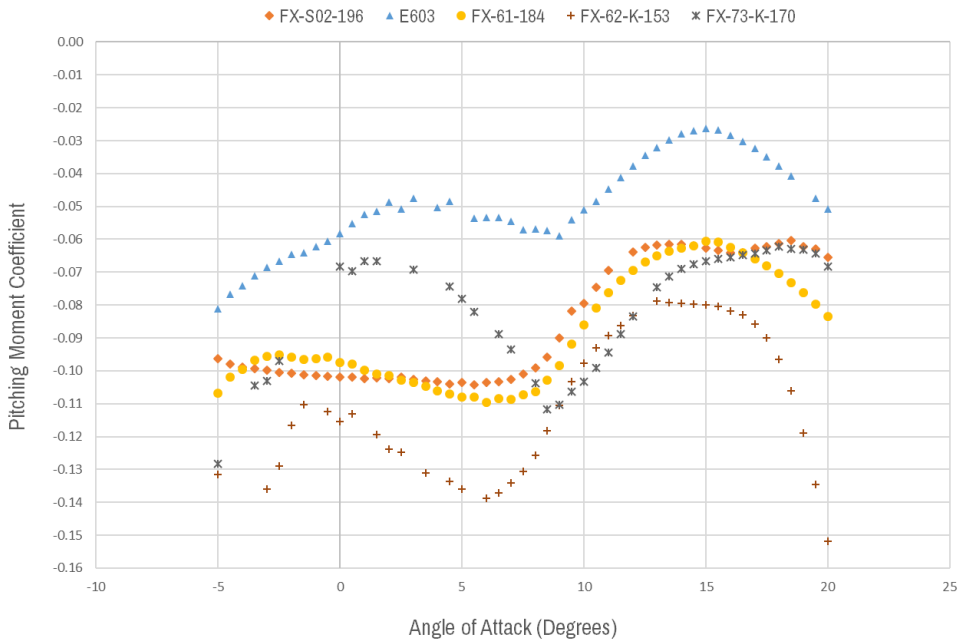

Figure 17. Pitching moment coefficients of root section airfoils changing with angle of attack

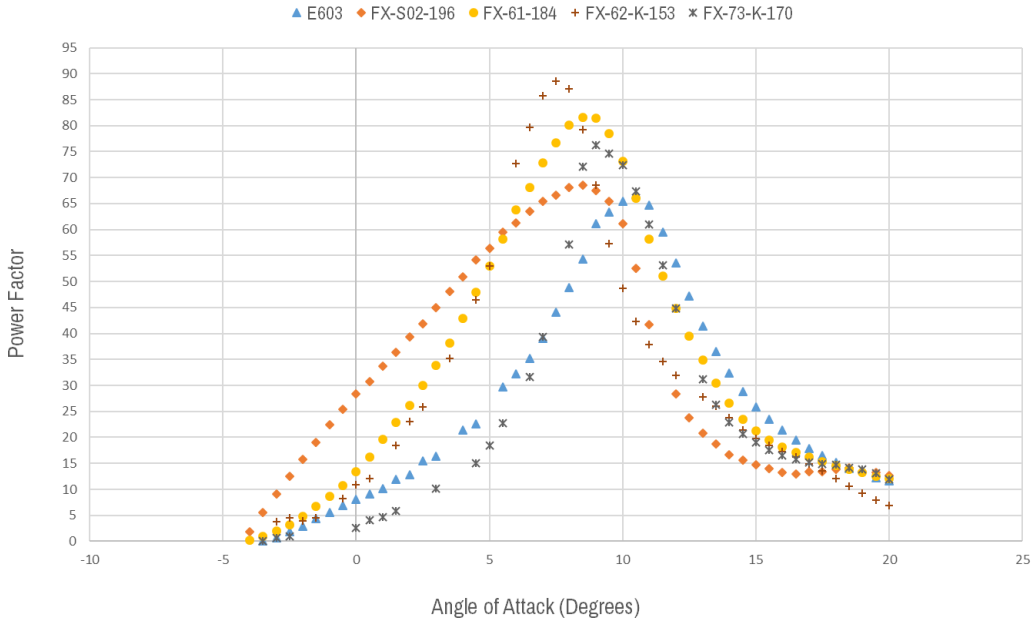

Figure 18. Power factors of root section airfoils changing with angle of attack

4. Conclusion

In this study, with the aim of comparison of airfoils in terms of sailplane aerodynamic performances, nine different airfoils were selected with respect to usage frequency at historical usage data. Additionally, airfoils were grouped with respect to their application trends in the historical usage data at root or tip sections of sailplane wing designs. For the comparison, firstly reliability verification

analyses of XFLR5 were performed and results were validated with the experimental data. Later on, nine different airfoils were analyzed under the same validated conditions. With the results of the analyses, which were at $2x10^5$ Reynolds number and from -5 to 20 degree angle of attack with 0.5 degree intervals, airfoils were scored from 1 to 5 with respect to determined criteria as stated in Table 4 and Table 5. Consequently, in terms of determined seven criteria, Wortmann FX S02-196 and FX Wortmann FX61-184 airfoils were equally found to be the most efficient airfoils for root section of a sailplane wing design among the selected five root section airfoils. Similarly, in terms of determined seven criteria, GOE 533 airfoil was found to be the most efficient airfoil for tip section of a sailplane wing design among the selected four tip section airfoils.

References

Deperrois, A. (2009). XFLR5 Analysis of foils and wings operating at low Reynolds numbers. *Guidelines for XFLR5*.

Drela, M. (1989). XFOIL: An analysis and design system for low Reynolds number airfoils. In *Low Reynolds number aerodynamics* (pp. 1-12). Springer, Berlin, Heidelberg.

Eppler, R., Somers, D. M. (1980). A computer program for the design and analysis of low-speed airfoils.

Thomas, F., Milgram, J. (1999). *Fundamentals of sailplane design* (Vol. 3). College Park, Maryland: College Park Press.

Gudmundsson, S. (2013). *General aviation aircraft design: Applied Methods and Procedures*. Butterworth-Heinemann.

Hansman, R. J., Craig, A. P. (1987). Low Reynolds number tests of NACA 64-210, NACA 0012, and Wortmann FX67-K170 airfoils in rain. *Journal of Aircraft*, *24*(8), 559-566.

Hasan, M., El-Shahat, A., Rahman, M. (2017). Performance Investigation of Three Combined Airfoils Bladed Small Scale Horizontal Axis wind Turbine by BEM and CFD Analysis. *Journal of Power and Energy Engineering*, *5*(05), 14.

Lasauskas, E., Naujokaitis, L. (2009). Analysis of three wing sections. *Aviation*, *13*(1), 3-10.

McGhee, R. J., Walker, B. S., and Millard, B. F. (1988). Experimental Results for Eppler E 387 Airfoil at Low Reynolds Numbers in the Langley Low-Turbulence Pressure Tunnel. *NASA Technical Memorandum-4062*.

Morgado, J., Vizinho, R., Silvestre, M. A. R., Páscoa, J. C. (2016). XFOIL vs CFD performance predictions for high lift low Reynolds number airfoils. *Aerospace Science and Technology*, *52*, 207-214.

Frati, S. (1946). The Glider. *Editore Ulrico Hoepli Milano, Milan, Italy*.

Sudhakar, S., Mishra, S., Ramesh, G., Madhavan, K. T., Ahmed, S. (2011). Experimental Studies on SM4308 Airfoil at Low Reynolds Numbers.

Vuruşkan, A., Özdemir, U., Yükselen, M.A., İnalhan, G. (2014, September). Dikey İniş Kalkış Yapabilen Bir İnsansız Hava Aracının (Turaç*) Aerodinamik Analizi. *V. ULUSAL HAVACILIK VE UZAY KONFERANSI*. Kayseri: Erciyes University.

Wahidi, R., Bridges, D. (2009, June). Experimental investigation of the boundary layer and pressure measurements on airfoils with laminar separation bubbles. In *39th AIAA Fluid Dynamics Conference* (p. 4278).

Xin, H. U. A., Rui, G. U., JIN, J. F., LIU, Y. R., Yi, M. A., Qian, C. O. N. G., ZHENG, Y. (2010). Numerical simulation and aerodynamic performance comparison between seagull aerofoil and NACA 4412 aerofoil under low-reynolds. *Advances in Natural Science*, *3*(2), 244-250.

URL-1: http://m-selig.ae.illinois.edu/ads/coord_database.html (Last Update: 12th of May 2018)